BRILL

IAWA Journal 36 (1), 2015: 3–21

iawa

STRUCTURE AND CHEMISTRY OF THE XYLEM OF ARBORESCENT SPECIES OF *BLECHNUM* FROM SOUTH AMERICA

María Luján Luna[1,2,*], **Juan Pablo Ramos Giacosa**[1,3], **Gabriela Elena Giudice**[1], **Paula Virginia Fernández**[3,4], **Marina Ciancia**[3,4] and **Mario C. N. Saparrat**[3,5,6,7]

[1]Cátedra Morfología Vegetal, Facultad de Ciencias Naturales y Museo, Universidad Nacional de La Plata, Paseo del Bosque s/n, (1900) La Plata, Argentina
[2]Comisión de Investigaciones Científicas de la Provincia de Buenos Aires
[3]Consejo Nacional de Investigaciones Científicas y Técnicas, Argentina
[4]Cátedra de Química de Biomoléculas, Facultad de Agronomía, Universidad de Buenos Aires, Av. San Martín 4456, C1417DSE CABA, Argentina
[5]Instituto de Fisiología Vegetal (INFIVE), Universidad Nacional de La Plata (UNLP)- CCT-La Plata, Consejo Nacional de Investigaciones Científicas y Técnicas (CONICET), Diag. 113 y 61, CC 327, (1900) La Plata, Argentina
[6]Instituto de Botánica Spegazzini, Facultad de Ciencias Naturales y Museo, UNLP, 53 # 477, (1900) La Plata, Argentina
[7]Cátedra de Microbiología Agrícola, Facultad de Ciencias Agrarias y Forestales, UNLP, 60 y 119, (1900) La Plata, Argentina
*Corresponding author; e-mail: lujanluna@fcnym.unlp.edu.ar

ABSTRACT

The xylem in three arborescent species of *Blechnum* section *Lomariocycas* was studied in detail using SEM, TEM, FT-IR spectroscopy and sugar composition analysis. The overall structure of root and rhizome metaxylem tracheids was similar in the three species analyzed, and characterized by mostly scalariform pitting of these multifaceted cells. Pit membrane thickness and porosity varied according to the stage of tracheid maturation. Approximately rounded deposits resembling vestures were observed in the outer pit apertures of some tracheids. Under TEM, thickenings like one-sided tori appeared on the tracheid side of tracheid-to-parenchyma contact walls; some parenchyma cells showed, in addition, features of transfer cells. As the increase in stature creates new constraints in terms of biomechanical support and water transport in plants, the characteristics found in *Blechnum* xylem might be related to optimization of conductive efficiency and safety. Chemical analyses of roots and rhizomes of *B. yungense* revealed similar levels of G-type lignin deposited in the xylem cell walls. Such lignin is the most common in ferns, including other arborescent genera. Preliminary analysis of cell wall polysaccharide composition of both root and rhizome xylem, yielded cellulose, xyloglucans and xylans with low amounts of mannans and pectins. The xylem of rhizomes had higher amounts of cellulose than root xylem. Our results are discussed in the context of functional and evolutionary aspects of xylem ferns.

Keywords: Arborescent ferns, tracheids, (pseudo)vestured pits, torus-like structures, transfer-cells, G-lignin, xyloglucans.

DOI 10.1163/22941932-00000081

INTRODUCTION

Water-conducting tissue of ferns consists typically of tracheids with scalariformly pitted walls and xylem parenchyma cells (Bierhorst 1960; Ogura1972; Gifford & Foster 1989). In rhizomes, xylem and phloem are arranged in "vascular bundles" or "meristeles" limited by an endodermis, whereas in roots the xylem occupies the central part of the stele cylinder (Ogura 1972). Presence of vessel elements has been reported in some fern taxa such as *Pteridium aquilinum* (Bliss 1939; Bierhorst 1960), *Equisetum* (Meyer 1920; Bierhorst 1958; Dute & Evert 1977), *Marsilea* (White 1961; Bhardwaja & Baijal 1977), *Actiniopteris radiata* (Singh *et al*. 1978), *Astrolepis* (Carlquist & Schneider 1997, 2007) and *Woodsia* (Carlquist & Schneider 1998, 2007). Extant ferns only form primary vascular tissues and do not develop a secondary vascular cambium (Gifford & Foster 1989; Rothwell & Karrfalt 2008).

In the last decades, phylogenetic studies have revealed a basal dichotomy within vascular plants, separating the lycophytes (Lycopodiophyta) from the euphyllophytes, the latter including ferns and seed plants (Kenrick & Crane 1997; Pryer *et al*. 2004; Smith *et al*. 2006; Christenhusz & Chase 2014). Extant ferns appear to be a monophyletic group characterized, among other features, by mesarch xylem (*i.e*., protoxylem differentiates first in the center of the vascular bundle) in their shoots (Ranker & Haufler 2008).

Information regarding ultrastructure and development of tracheary elements in ferns, as well as of primary and secondary cell wall chemistry, is scarce (Friedman & Cook 2000; Luna *et al*. 2010). Scanning electron microscopy (SEM) studies performed on tracheids of some ferns provided detailed information of their wall structure (*i.e*. pitting, cell wall thickenings), and revealed the ultrastructure of their pit membranes (Carlquist & Schneider 2007 and literature cited therein; Luna *et al*. 2008, 2010). Transmission electron microscopy (TEM) studies have been limited to tracheids of the lycophyte *Huperzia* and of few ferns such as *Botrychium*, *Equisetum* and *Asplenium* (Cook & Friedman 1998; Morrow & Dute 1998; Friedman & Cook 2000; Luna *et al*. 2010). In *Huperzia* and *Equisetum*, the secondary cell walls exhibited the degradation-prone and degradation-resistant layers commonly found in tracheids of early fossil vascular plants. For *Botrychium*, Morrow and Dute (1998) reported the development of a torus in the inter-tracheid and tracheid-to-parenchyma pit membranes. Pit membrane hydrolysis was observed in *Huperzia* and *Asplenium* (Cook & Friedman 1998; Luna *et al*. 2010).

According to phylogenetic studies based on molecular data the genus *Blechnum* L., which is the object of our study, diversified in the late Cretaceous (Pryer *et al*. 2004). It is cosmopolitan in distribution, with approximately 150–200 species around the world. Within *Blechnum*, section *Lomariocycas* (J. Sm.) C.V. Morton groups species with arborescent habit and upright rhizomes 0.30–2 meters heigh (Morton 1959; Ramos Giacosa 2008).

Different strategies have been developed in land plants to stay erect as they grow, such as development of lignified tissues (*i.e*. xylem), and/or persistence of leaf-bases. In ferns with an arborescent habit, girth and strength of the rhizome are provided by persisting leaf bases and a mantle of adventitious intertwining roots (Donoghue 2005;

Simpson 2010). In the absence of secondary growth, cell walls of parenchyma and/or sclerenchyma tissues help maintain the erect habit of tree ferns.

In vascular plants, polysaccharide-based walls of water-conducting cells are strengthened by impregnation with lignin (Boyce *et al*. 2004; Weng & Chapple 2010). According to Boyce *et al*. (2004), fine-scale patterning of lignin deposition in water-conducting cells varies among vascular plants; for example ferns possess tracheids with weak primary wall lignification and more strongly lignified secondary walls.

Within ferns, biochemical data on lignin composition is only available for a few taxa such as *Cyathea*, *Dennstaedtia*, *Equisetum*, *Dryopteris, Phyllitis* and *Pteridium*, among others (Kawamura & Higuchi 1964; Logan & Thomas 1985; Espiñeira 2008; Espiñeira *et al*. 2011). Lignin found in ferns contained mostly G units (guaiacyl) and less frequently S units (syringyl).

The aim of this study was to investigate anatomically and chemically the xylem in three arborescent species of *Blechnum* sect. *Lomariocycas*. This information is discussed in the context of adaptive strategies and evolution of the water-conducting tissue in plants.

MATERIALS AND METHODS

Living specimens of three arborescent species of *Blechnum* were collected at their natural habitats: *B. magellanicum* (Desv.) Mett. (Parque Nacional Lago Puelo, Provincia de Chubut, Argentina), *B. schomburgkii* (Klotzsch) C. Chr. (Gruta de los Helechos, Departamento Tacuarembó, Uruguay) and *B. yungense* Ramos Giacosa (Parque Nacional Calilegua, Provincia de Jujuy, Argentina) (Ramos Giacosa 2010). All of them have upright stems (rhizomes), which reach a height of 50–60 cm and a diameter of c. 30 cm (Fig. 1–2). Voucher specimens have been deposited in the LP herbarium.

Due to the greater availability of materials, *Blechnum yungense* was selected as representative for chemical and TEM studies.

Figure 1–2. General view of a specimen of *Blechnum* sect. *Lomariocycas*. – 1: *Blechnum magellanicum* growing in Lago Puelo National Park (arrow). – 2: External appearance of the rhizome (arrow).

Anatomy

Portions of roots and rhizomes were prepared for light microscopy (LM), scanning electron microscopy (SEM) and transmission electron microscopy (TEM). Prior to fixation cortical tissue was removed from most samples for best results.

Specimens for LM were fixed in formaldehyde-acetic acid-alcohol, dehydrated through an ethanol series and embedded in Paraplast. Sections (8–12 μm thick) were double stained with safranin-fast green (Johansen 1940). Part of the material was macerated according to Jeffrey's technique (Jeffrey 1917). Samples were placed in the solution for 12 hours at room temperature, and then washed with distilled water. Preparations were stained with safranin and observed under a Nikon Photolab 2 light microscope.

For SEM study, material was treated according to the methods of Dute *et al*. (1992) and Jansen *et al*. (2008). Transverse and longitudinal sections of roots and rhizomes were split using a razor blade. Sections were placed in 80% ethanol, then in 90% ethanol, followed by absolute ethanol and finally allowed to air dry. Samples were attached to aluminum stubs using double sticky tape, air dried and sputter-coated with gold-palladium. Observations were made in a JEOL, JSM-35 CF scanning electron microscope.

For TEM analysis, samples 3–5 mm in length were fixed in a 2% glutaraldehyde solution in 0.1 M phosphate buffer (pH 7.2–7.4) and vacuum-infiltrated at room temperature for 4 hours; then rinsed three times in the same buffer and post-fixed for 2 hours in 1% osmium-tetroxide under vacuum at room temperature. Specimens were then dehydrated in an ethanol-acetone series and embedded in Spurr's resin. Sections (70–90 nm) were stained with uranyl acetate followed by lead citrate and examined with a Zeiss T-109 transmission electron microscope.

Fourier Transform Infra Red (FT-IR) spectroscopy and sugar composition analysis of the cell walls of Blechnum yungense xylem

For chemical analysis, xylem was detached from rhizomes and roots using a razor blade and then processed according to Espiñeira *et al*. (2011). Briefly, each sample was dried at 80 °C overnight and ground into fine powder with an agate mill until a good degree of homogeneity was reached (cf. Saparrat *et al*. 2010). From each powder, cell walls were prepared by a Triton X-100 washing procedure, which included as last steps a washing with ethanol (three times) followed by an additional one with diethyl ether (also three times). The resulting crude cell wall material of each sample was used for Fourier Transform Infra Red (FTIR) and sugar composition analysis.

For FTIR, 2 mg of each powder was dried, mixed with 200 mg KBr, and pressed into a 13-mm pellet, which was then scanned from 4,000 to 400 cm^{-1} averaging 64 scans at 1 cm^{-1} interval with a resolution of 4 cm^{-1}. The spectra obtained were processed and analyzed by using OMNIC software (Thermo Nicolet, Madison, Wl, USA) according to Saparrat *et al*. (2010). Bands selected as index peaks reflecting functional groups associated with the cell walls were assigned according to Saparrat *et al*. (2009, 2010). On the resultant FT-IR spectra, which were previously corrected by automatic subtraction of the background, several parameters related to degree of lignification (Hinterstoisser

et al. 2001), the relative lignin content (Dobrică *et al*. 2008) and different ratios such as lignin : carbohydrate one, carbonyl : carbohydrate one and S : G one (Bechtold *et al*. 1993; Dorado *et al*. 1999) were estimated.

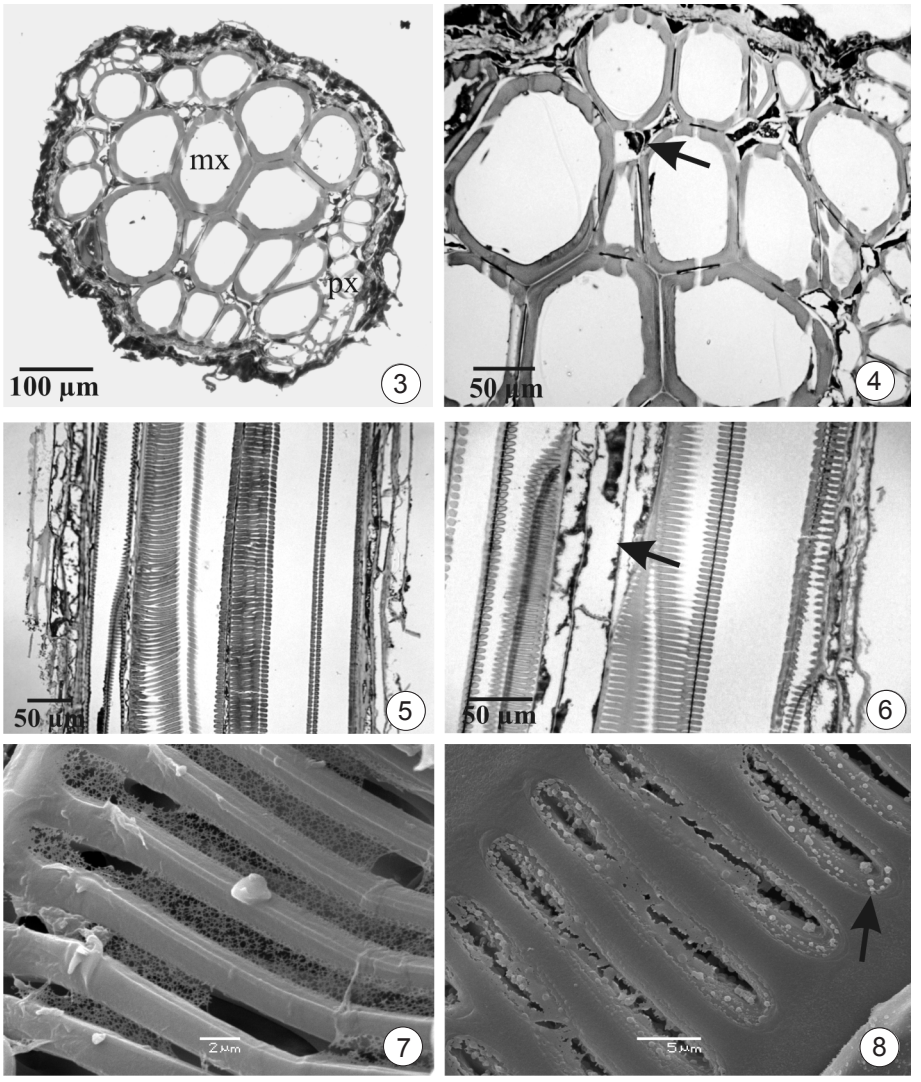

Figure 3–8. Light micrographs (LM) and scanning electron micrographs (SEM) of root. – 3–6: LM. – 3: Transverse section (TS) showing diarch actionostele (mx: metaxylem; px: protoxylem). – 4: TS, detail of xylem zone with few metaxylem tracheids and scarce parenchyma cells (arrow). – 5: Longitudinal section (LS) through a portion where metaxylem tracheids with scalariform pitting are evident. – 6: LS, a more detailed view showing xylem parenchyma (arrow) interspersed with metaxylem tracheids. – 7 & 8: SEM. – 7: Porose pit membrane at a later stage of hydrolysis. – 8: Rounded deposits (arrow) on outer pit apertures of a tracheid.

Total sugar content was analyzed by the PhOH–H_2SO_4 method (Dubois *et al*. 1956) adapted for insoluble material (Ahmed & Labavitch 1977). Uronic acid content was measured according to Filisetti-Cozzi & Carpita (1991). Monosaccharide composition of the two samples was determined by reductive hydrolysis and acetylation of the sugar mixtures according to Stevenson and Furneaux (1991) (method A). Alternatively, hydrolysis was carried out in 100 % TFA for 1 h at 37 °C, followed by dilution of the acid to 80 %, heating at 100 °C for 1 h, and further dilution to 2 M to achieve the regular hydrolysis conditions for insoluble polysaccharides (Morrison 1988); the

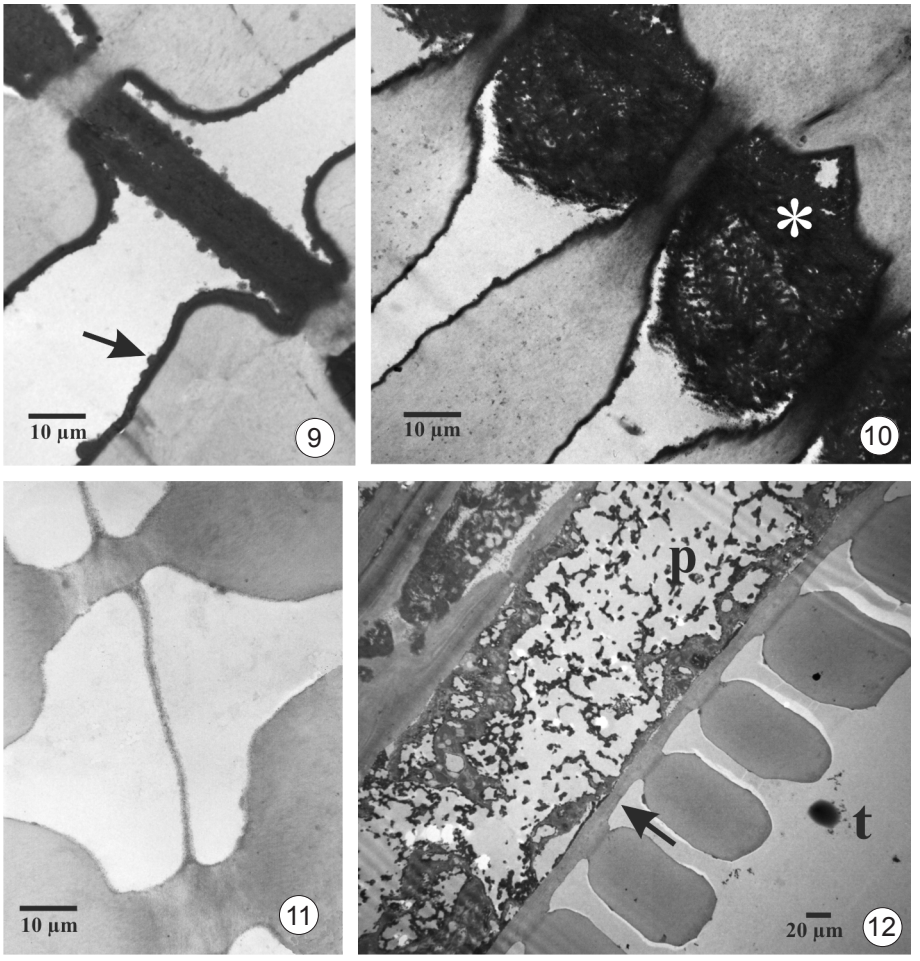

Figure 9–12. Transmission electron micrographs (TEM) of root. – 9: Longitudinal view of portions of tracheids showing thickened pit membrane and electron dense deposits on the lumen side (arrow). – 10: Detail of pit membrane composed of loosely interwoven microfibrils that give rise to small spaces between them (asterisk). – 11: Thinner inter-tracheary pit membrane. – 12: Tracheid (t) to parenchyma (p) contact walls showing bordered pits on the tracheid side (arrow). Parenchyma cells have primary walls only.

sugar mixture was derivatized to the corresponding alditol acetates (method B). GLC of the alditol acetates were carried out on an Agilent 7890 gas-liquid chromatograph (Avondale PA, USA) equipped with a flame ionization detector and fitted with a fused silica column (0.25 mmi.d. × 30 m) WCOT-coated with a 0.20 μm film of SP-2330 (Supelco, Bellefonte PA, USA). Chromatography was performed from 200 °C to 230 °C at 1 °C min^{-1}, followed by a 30-min hold. N_2 was used as the carrier gas at a flow rate of 1 ml min^{-1} and the split ratio was 50 : 1. Injector and detector temperatures were 240 °C and 300 ºC, respectively.

RESULTS

Anatomy and ultrastructure

Roots

In transverse section roots show a diarch actinostele, with exarch xylem (*i.e.* protoxylem differentiate in the periphery of the xylem cylinder) and c. 15–18 metaxylem tracheids, interspersed with few parenchyma cells (Fig. 3–6). Mean metaxylem tracheid diameter is 86 μm (60–102) and mean length is 942 μm (880–1050). Vascular tissues (xylem and phloem) are surrounded by pericycle and endodermis.

Under SEM inter-tracheid pit membranes are intact in most cases, and thus, torn or absent pit membranes were considered artifacts. Different degrees of porosities are observed, presumably in association with the stage of tracheid development. Porose to reticulate pit membranes are found in tracheids regarded as more mature (Fig. 7). These pores are absent in tracheid-to-parenchyma pit membranes. In some instances, rounded deposits are found on the outer apertures of inter-tracheid pits (Fig. 8).

Secondary walls of tracheids have a homogeneous appearance under TEM. In younger cells, a dark layer outlining the cell lumen is visible, along with irregular to rounded deposits, likely remnants of cytoplasm (Fig. 9). Inter-tracheid pit membranes show a variation in thickness that correlates to their stage of maturation. Thicker pit membranes with randomly oriented and loosely interwoven microfibrils occur between presumably younger tracheary elements (Fig. 10). In older tracheids membranes are thinner due to advanced cell wall hydrolysis (Fig. 11). The scarce xylem parenchyma cells exhibit primary walls only (Fig. 12).

Rhizomes

In transverse sections, rhizomes exhibit a dictyostele with a ring of vascular bundles or "meristeles", which are surrounded by a pericycle (2–4 layers of cells) and an endodermis with Casparian strips in their radial walls (Fig. 13–14). Xylem maturation is mesarch; mean metaxylem tracheid diameter is 46 μm (28–63) and mean length is 1564 μm (1047–2180). The phloem is positioned external to the xylem, in groups.

Tracheids are interspersed with parenchyma cells (Fig. 15–16). Parenchyma is relatively abundant, so that contacts between parenchyma and tracheids are very frequent.

Under SEM, metaxylem tracheids show several facets with scalariform bordered pits; facets with oval or circular bordered pits are also present (Fig. 17–20). Inter-tracheary

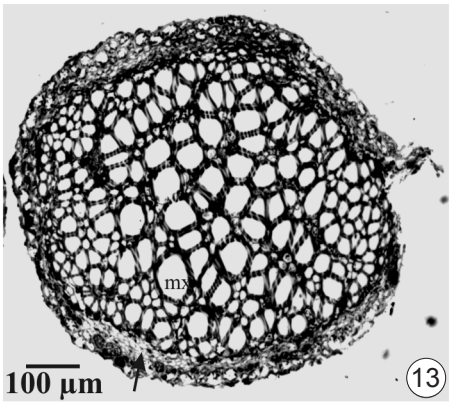

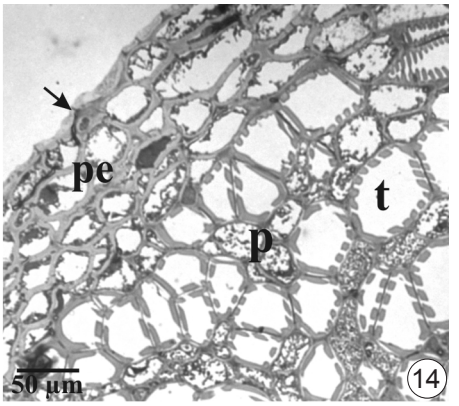

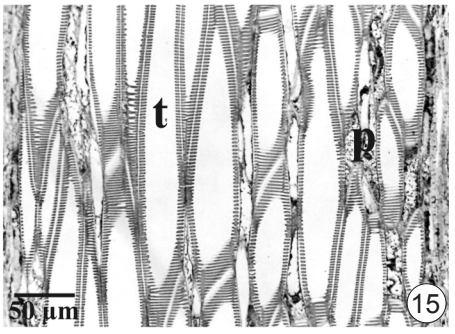

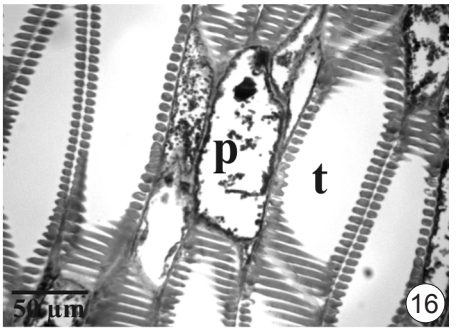

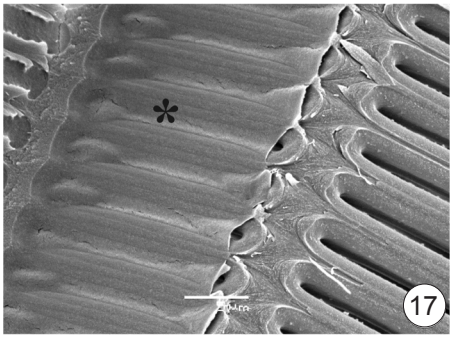

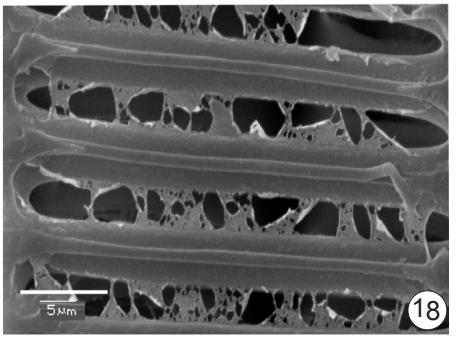

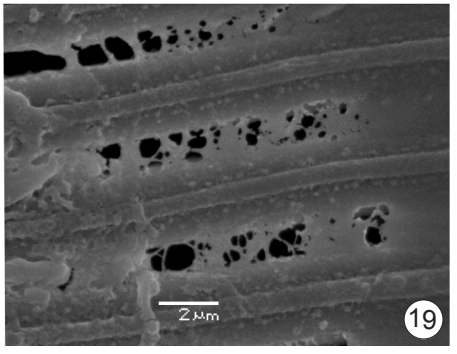

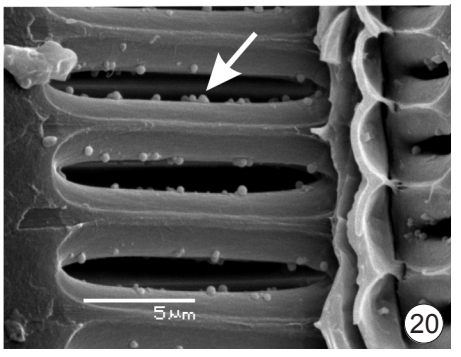

pit membranes are present in lateral walls as well as in end walls and their absence in excised samples is an artifact due to tissue processing (Fig. 17). Although pit membranes are usually non-porous, we observed pit membrane sectors with different degrees of porosity (Fig. 18–19). In some instances rounded deposits are observed in the outer pit apertures of tracheids (Fig. 20).

Under TEM, secondary walls of tracheids have a homogeneous appearance whereas parenchyma cells have only primary walls (Fig. 21–22). As mentioned for the roots, inter-tracheid pit membranes show a variation in thickness, presumably in association with their developmental stage (Fig. 23–25).In young tracheids, the lumen side appears outlined by a dark layer and electron-dense deposits, attributable to residual cytoplasm (Fig. 23).Other structures, also electronically dense and rounded in shape, are observed in association with the pits in presumed mature tracheids (Fig. 26–27). Pit membrane thickenings with an electron-dense coating are registered on the tracheid side of tracheid-to-parenchyma contact walls (Fig. 28–30). In some samples, it is possible to observe that the thickened zone is traversed by less electron-dense structures resembling plasmodesmata (Fig. 29). Cell wall ingrowths typical of transfer cells sometimes occur in parenchyma cells adjacent to tracheids (Fig. 31).

Overall chemical characterization of tracheid walls of Blechnum yungense

The FTIR spectra of cell wall samples from roots and rhizomes show a similar pattern (Fig. 32), typical for lignocellulose substrates with several peaks in the finger print region (800–1800 cm^{-1}) (Table 1). However, absorbance was higher for rhizome than for root samples. The degree of lignification and the relative lignin content in each sample as well as the ratios S units/G units, lignin/carbohydrate and carbonyl : carbohydrate are shown in Table 2. Whereas a similar S units/G units ratio typical of G-lignin is detected in both samples (root and rhizome), a higher relative content of lignin is estimated for the rhizome xylem sample.

Total sugars content is similar for both root and rhizome xylem samples (40.3 ± 2.1% and 42.2 ± 3.0 % respectively). After performing reductive hydrolysis and derivatization, we determined the monosaccharide composition of pectins and some hemicelluloses (method A). Using stronger conditions of hydrolysis (method B) we hydrolized all hemicelluloses and cellulose. Accordingly, a higher proportion of glucose is found in the monosaccharide mixture obtained by method B for both xylem samples, with

←

Figure 13–20. Light micrographs (LM) and scanning electron micrographs (SEM) of rhizome. – 13–16: LM. – 13: TS of a meristele or vascular bundle (mx: metaxylem; the arrow indicates the position of the phloem). – 14: Detail which shows that parenchyma cells (p) are relatively abundant between tracheids (t). Vascular tissues are surrounded by the pericycle (pe) and the endodermis (arrow). – 15: LS of a meristele showing scalariformly pitted metaxylem tracheids (t) interspersed with parenchyma cells (p). – 16: Xylem parenchyma cells (p) in detail. – 17–20: SEM. – 17: Portion of a tracheid with intact, nonporose pit membrane at left (asterisk). – 18: Portion of a tracheid with torn pit membrane, which probably becomes weaker as a consequence of advanced hydrolysis. – 19: Portion of a tracheid with small pores and rounded deposits on the outer pit aperture. – 20: Detail of rounded deposits (arrow) on the outer pit aperture.

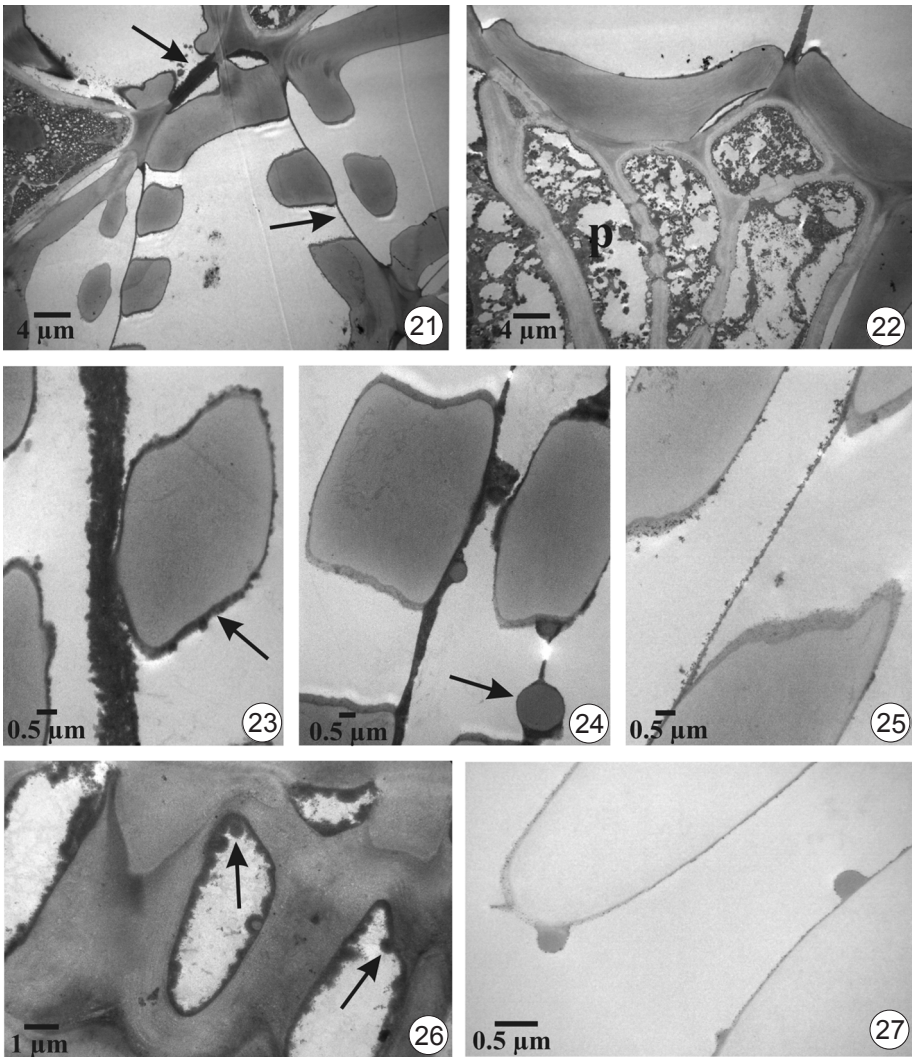

Figure 21–27. Transmission electron micrographs (TEM) of rhizome. – 21: Portion of meristele in TS showing a different thickness of inter-tracheary pit membranes (arrows). – 22: Detail of xylem parenchyma cells (p) with primary walls only. – 23: Thickened inter-tracheary pit membrane between presumably younger tracheids. An electron dense layer is also observable on the tracheid's walls (arrow). – 24: Relatively thinner pit membrane in which hydrolysis apparently has begun. Rounded structures with similar contrast as the cell wall are observed (arrow). – 25: A more advanced stage of hydrolysis showing an even thinner pit membrane. – 26: An assumed younger tracheid with electron dense deposits (arrows) attributable to residual of cytoplasm. – 27: Rounded electron dense protuberances in the wall of a putative mature tracheid.

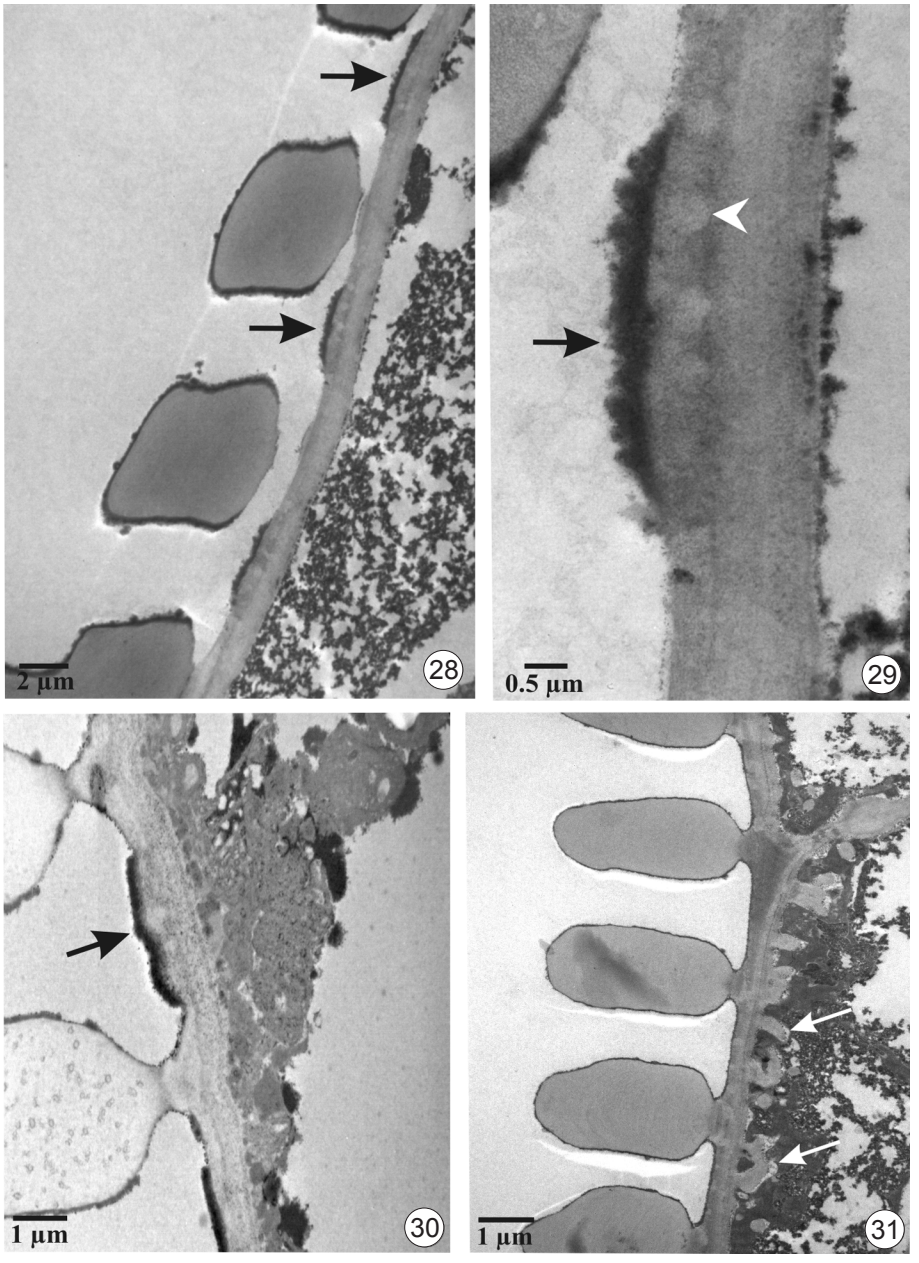

Figure 28–31. Transmission electron micrographs (TEM) of rhizome. – 28: Tracheid-to-parenchyma contact walls showing cell wall thickenings on the tracheid side (arrows). – 29: Detail of a thickened zone where electron dense deposits (arrow) and rounded structures resembling plasmodesmata (arrowhead) are observed. – 30: A more thickened condition, also with electron dense deposits on the lumen side of the tracheid (arrow). – 31: Tracheid-to-parenchyma contact walls showing cell wall ingrowths of parenchymatic cell (arrows).

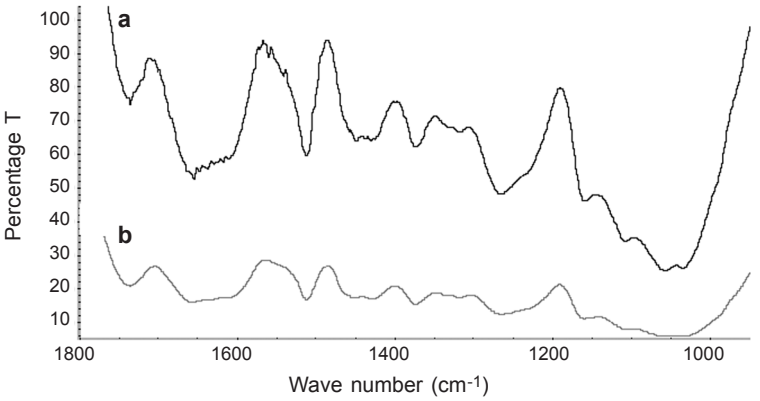

Figure 32. Fourier transform infrared (FTIR) transmission spectra of xylem cell walls from *Blechnum yungense*: a, rhizome; b, root.

Table 1. Assignment of IR absorption bands in the spectra of xylematic cell walls of root and rhizome of *Blechnum yungense*.

Wavenumber (cm^{-1})	Assignment (functional groups)
IR cellulose bands	
899	C-H deformation
1035	C-C, C-O, O-C-H bonds of pyranoside rings
1058	C-C, C-O, O-C-H bonds
1108	C-C, C-O bonds, pyranoside ring
1160	glycosidic C-O-C vibration
1318	CH_2 stretch
IR lignin bands	
1266	C-O of the guaiacyl ring
1318	C-O of the syringyl ring
1375	CH-deformations of acetyl groups
1450–60	C-H deformation (methyl and methylene) in monolignols
1510	aromatic skeletal vibrations
1611	aromatic skeletal vibrations
IR protein bands	
1625	amide I (N-H bending)
IR non-cellulosic polysaccharides bands	
810–820	C1-H bonds and rings probably associated with rhamnogalacturonan-like compounds
899	C1-H vibration in hemicellulose
1630	carboxylate groups of pectins
1660	conjugated carbonyl groups of pectins
1736	non-conjugated carbonyl groups of pectins and hemicelluloses (xylans)

Table 2. Parameters obtained from the FTIR data.

		Rhizome	Root
Degree of lignification[a]	I_{1510}/I_{895}	4.43	3.75
S/G ratio[b]	I_{1327}/I_{1271}	0.72	0.73
Lignin content[c]	(%)	32.2	31.7
Lignin/carbohydrate ratio	I_{1510}/I_{1373}	1.05	0.93
	I_{1510}/I_{1161}	0.79	0.71
Carbonyl/carbohydrate ratio	I_{1738}/I_{1373}	0.78	0.73
	I_{1738}/I_{1161}	0.59	0.56

[a] According to Hinterstoisser *et al*. (2001).
[b] According to del Río *et al*. (2007).
[c] The lignin content was determined from the C = C band intensity (through the height of the 1505 cm^{-1} band) using the following non-linear equation:
% lignin = -1.23 + (193.4 × band intensity) – (279.8 × band intensity^2) (Dobrică *et al*. 2008).

Table 3. Monosaccharide composition of xylem from root and rhizome of *Blechnum yungense* after a mild (Method A) and strong (Method B) hydrolysis treatments.

Structure	Hydrolysis method	Monosaccharide composition (mols %)						
		Ramnose	Fucose	Arabinose	Xylose	Manose	Galactose	Glucose
Rhizome	A	6	1	13	36	13	13	18
	B	2	Tr[a]	8	19	11	8	52
Root	A	4	1	7	39	16	13	20
	B	2	1	9	24	12	10	42

[a]Tr = traces.

higher levels of glucose release from the rhizome compared to the root. Furthermore, both hydrolysis methods show that there are no statistically significant differences in the monosaccharide composition and relative abundance in the two organs (Table 3). Xylose is the major monosaccharide component obtained by method A; mannose is also detected in important quantities.

The content of uronic acids is low in both root (1.7%) and rhizome (1.9%) samples. The presence of small amounts of rhamnose suggests that these uronic acids derive mostly from pectins.

DISCUSSION

The general structure of the tracheids under LM and SEM is broadly similar in the three species analyzed, and coincides with that described in other ferns with varied growth habits and ecological preferences (Carlquist & Schneider 2007; Luna *et al*. 2008, 2010). Therefore, we focus our discussion on some adaptive features that may facilitate or regulate water movement in species with arborescent habit that creates

new demands and constraints in terms of biomechanical support and water transport (Meyer-Berthaud *et al*. 2010). Watkins *et al*. (2010) emphasized that most ferns have limited path lengths for water transport between roots and leaves, suggesting that the apparent lack of innovations in xylem cells may reflect architectural constraints.

One of the characters related to water conductivity in plants is tracheid (or vessel) diameter (Niklas 1985). Although the relationship between tracheid diameter and conductivity is not an aim of this study, it seems appropriate to make some comments emerging from our investigation. For the *Blechnum* species analyzed here, mean metaxylem tracheid diameter in the rhizome (based on the maximum width of the cell lumen, according to Niklas 1985) was under 50 μm, which coincides with Veres' findings in other species of *Blechnum* with different growth habits (Veres 1990). In our study, the diameter of most tracheids is near 46 μm whereas a few reach 63 μm. Veres (1990) analyzed the relationship between tracheid diameter and water conductivity in horizontally stemmed and climbing species of *Blechnum*, and found larger conductivities in association with greater numbers of larger tracheids (near 100 μm in diameter). We can hypothesize *a priori* that vertical stems of *Blechnum* would not show higher conductivity than species with horizontal or climbing stems. This would be consistent with the statement by Veres (1990), in that elongated stems are found to exhibit the largest hydraulic conductivities, whereas smaller conductivities are associated with the erect habit. Watkins *et al*. (2010) also claimed an association between hydraulic conductivity and life forms in ferns, rather than with the habitat where they grow. Since in the species studied here the tracheids have similar diameters and live in different habitats, we might conclude that the environment does not have an influence on hydraulic conductivity.

Other features related to water flow in plants are pit membrane thickness and porosity, which limit the spread of embolisms and vascular pathogens in the xylem (Choat *et al*. 2008; Nardini *et al*. 2011). In the species analyzed here, we observed partial hydrolysis of root and rhizome inter-tracheid pit membranes during cell maturation, as occurs in other ferns and in the lycophyte *Huperzia* (Cook & Friedman 1998; Morrow & Dute 1998; Carlquist & Schneider 2007; Luna *et al*. 2008, 2010). As a result, pit membranes appeared thinned and porous, as postulated in general for fern tracheids (Carlquist & Schneider 2007). This phenomenon was characterized by a general thinning of the pit membrane and the presence of pores as observed by TEM. Loss of some or all of the matrix material during maturation results in porous membranes that reduce hydraulic resistance but increase vulnerability to embolism (O'Brien 1970; Choat *et al*. 2008).

In some samples (viewed using SEM) roughly rounded deposits were noted sporadically in the outer pit apertures of tracheids of both roots and rhizomes. They were also detectable as electron-dense deposits with TEM. The origin of these structures was not analyzed in this work, although at times they resembled vestures. Vestures were first described by Bailey (1933) as outgrowths from the secondary cell wall. It is known that some artifacts produced by extraneous or coagulated material may be confused with vestures, thus they are called "pseudovestures" (Bailey 1933; Jansen *et al*. 1998). According to Jansen *et al*. (1998), pseudovestures are soluble in mild solvents and they are not an integral part of the cell wall. Due to the rare occurrence of the deposits found

in *Blechnum* and the lack of information on the existence of vestured pits in ferns, other methods than those used in this work are necessary to determine their origin and nature.

Under TEM, thickenings resembling one-sided tori appeared frequently on the tracheid side of tracheid-to-parenchyma blind pits. These thickenings were covered by an electron-dense layer likely derived from cytoplasm remnants. Our observations are in agreement with the analysis of *Botrychium* by Morrow and Dute (1998). However, in this species, tori developed also in inter-tracheary pit membranes possibly preventing embolisms in the upright stems of *Botrychium*.

In the case of *Blechnum*, there are no such thickenings in the inter-tracheid pit membranes. This is in agreement with the observation that fern tracheids generally possess the ancestral homogeneous pit membrane that confers much greater pit area resistance than the torus-margo pitting typical of conifer tracheids (Pittermann *et al*. 2011). Further studies are necessary to understand the possible role of the thickenings observed on the tracheid side of tracheid-to-parenchyma contact walls in rhizomes of *Blechnum*.

In addition, we observed that some parenchyma cells in contact with tracheids showed features of transfer cells. It is known that transfer cells play an important role in transferring solutes over short distances (Gunning 1977). Their presence is generally correlated with the existence of intensive solute fluxes, in either inward (uptake) or outward (secretion) directions, across the plasma membrane (Evert 2006). Sperry (2003) stated that during land colonization, the high levels of atmospheric carbon dioxide may have favored systems with relatively low hydraulic conductance and at the same time, high ability to store water in cells as parenchyma. Thereby, the vertical stem habit in ferns may have been favored by the development of adaptive features that regulate water flow, such as torus in tracheid-to-parenchyma pit membranes as well as transfer cells, in relationship to intensive short-distance solute transfer. As Nardini *et al*. (2011) suggested, xylem hydraulic conductance regulation and maintenance seems to require metabolic activity of axial and radial xylem parenchyma and/or phloem. The role of the xylem parenchyma cells in the stems of ferns requires further analysis. We are currently analyzing taller tree ferns belonging to the genera *Alsophila* and *Cyathea* (2–3 or more meters in height) to further understand early strategies of water flow in plants.

On the basis of infra-red spectra, Kawamura and Higuchi´s (1964) classified fern lignin as a subdivision of the gymnospermous lignin, since most ferns have a G-type including arborescent taxa such as *Alsophila* and *Cyathea*. In agreement with Kawamura and Higuchi (1964), we detected an enrichment of G-type lignin in xylem of both root and rhizome of *Blechnum yungense*.

It has become evident that cell wall composition is a very relevant feature in the phylogenetic diversification of embryophytes (Espiñeira *et al*. 2011). Gymnospermous lignins are typically composed of G units, with a minor proportion of H units. In contrast, lignins of angiosperms, gnetophytes and some lycophytes, like *Selaginella*, are characterized by similar levels of G and S units. Since S lignins are present from non-vascular basal land plants, such as liverworts, to lycopods, gymnosperms and ferns,

Espiñeira *et al*. (2011) suggested that the presence of S lignin is an ancestral character in land plant evolution.

In angiosperms S lignin is often associated with fibers, which have an important role in mechanical support, and some authors have hypothesized that S lignin may be superior to G lignin in its ability to strengthen cell walls (Weng *et al*. 2008). Logan and Thomas (1985) highlighted the fact that, in the ferns such as *Dennstaedtia bipinnata* and *Lygodium circinatum*, substantial amounts of syringyl aldehyde were found in association with well-developed sclerotic sheaths in their steles. In addition, Weng *et al*. (2008) found that in *Selaginella*, S lignin accumulates primarily in the sclerified cortical cells, suggesting that these cells may play an important role in support of the plant body. Our chemical studies conducted only on isolated portions of xylem of *Blechnum yungense* provide additional evidence that the G-type lignin is common in the tracheary elements of ferns. However, it would be interesting to determine whether a different type of lignin accumulates in the cortical tissues of these ferns.

In addition, neither the carbohydrate and uronic acid relative contents, nor the monosaccharide composition of the cell walls show important differences between root and rhizome, with the exception of a higher amount of cellulose in xylem from the rhizome. For both organs, small amounts of uronic acids and rhamnose likely derive from pectins mostly rhamnogalacturonan I. The low content of galactose and arabinose could derive from rhamnogalacturonan I side chains. The presence of xyloglucans in primary cell wall from leaves of ferns, including *Blechnum* species, has been previously reported (Silva *et al*. 2011). Consistently, we have detected large amounts of xylose, suggesting that xyloglucans are the main cross-linking glycans in xylem cell walls of *B. yugense*, just like in type I cell walls of dicots, many monocots and some ferns (Carpita & Gibeaut 1993; Albersheim *et al*. 2011). Alternatively, the high relative content of xylose could be due to the presence of xylans. According to the traditional cell wall model (Albersheim *et al*. 2011), xylans would derive from secondary walls. The relatively abundant pool of mannose could derive from mannans as previously reported for cell walls of leaves of *B. polypodioides* (Silva *et al*. 2011). A more comprehensive biochemical analysis of the xylem tissue of *B. yungense* will be critical to understand functional and evolutionary aspects of the arborescent habit in ferns.

ACKNOWLEDGEMENTS

The authors wish to thank the staff of the National Parks Calilegua, Province of Jujuy and LagoPuelo, Province of Chubut, Argentina, for their collaboration in sample collection. To Professor Marisa Otegui, Departments of Botany and Genetics, University of Wisconsin-Madison for critically reading the manuscript. We are also grateful to the editor Pieter Baas, the reviewer Sherwin Carlquist and an anonymous reviewer, for their valuable suggestions that improved the quality of this manuscript. This study was supported by the Research Projects of Universidad Nacional de La Plata, Argentina (N/610), CONICET PIP 878 and PIP 391.

REFERENCES

Ahmed AER & Labavitch JM. 1977. A simplified method for accurate determination of cell wall uronide content. J. Food Biochemistry 1: 361–365.

Albersheim P, Darvill A, Roberts K, Sederoff R & Staehelin A. 2011. Plant cell walls: from chemistry to biology.Garland Science, Taylor & Francis Group, New York, USA.

Bailey IW. 1933. The cambium and its derivative tissues. VIII. Structure, distribution and diagnostic significance of vestured pits in dicotyledons. J. Arnold Arbor. 14: 259–273.

Bechtold R, González AE, Almendros G, Martínez MJ & AT Martínez. 1993. Lignin alteration by Ganoderma australe and other white-rot fungi after solid-state fermentation of beech wood. Holzforschung 47: 91–96.

Bhardwaja TN & Baijal J. 1977.Vessels in rhizome of *Marsilea*. Phytomorphology 27: 206–208.

Bierhorst DW. 1958. Vessels in *Equisetum*. Amer. J. Bot. 45: 534–537.

Bierhorst DW. 1960. Observations on tracheary elements. Phytomorphology 10: 249–305.

Bliss MC. 1939. The tracheal elements in the ferns. Amer. J. Bot. 26: 620–624.

Boyce CK, Zwieniecki MA, Cody GD, Jacobsen C, Wirick S, Knoll AH & Holbrook NM. 2004. Evolution of xylem lignification and hydrogel transport regulation. Proc. Natl. Acad. Sci. USA. 101: 17555–17558.

Carlquist S & Schneider EL. 1997. SEM Studies on vessels in ferns. 4. *Astrolepis*. Amer. Fern J. 87: 43–50.

Carlquist S & Schneider EL. 1998. SEM Studies on vessels in Ferns. 6. *Woodsia ilvensis* with comments on vessel origin in ferns. Flora 193: 179–185.

Carlquist S & Schneider EL. 2007. Tracheary elements in ferns: new techniques, observations, and concepts. Amer. Fern J. 97: 199–211.

Carpita NC & Gibeaut DM. 1993. Structural models of primary cell walls in flowering plants: consistency of molecular structure with the physical properties of the walls during growth. Plant J. 3: 1–30.

Choat B, Cobb A & Jansen S. 2008. Structure and function of bordered pits: new discoveries and impacts on whole plant hydraulic function. New Phytol. 177: 608–626.

Christenhusz MJM & Chase MW. 2014. Trends and concepts in fern classification. Ann. Bot. 113: 571–594.

Cook ME & Friedman WE. 1998. Tracheid structure in a primitive extant plant provides an evolutionary link to earliest fossil tracheids. Int. J. Pl. Sci. 159: 881–890.

Del Río JC, Gutiérrez A, Rodríguez IM, Ibarra D & Martínez AT. 2007. Composition of non-woody plant lignins and cinnamic acids by Py-GC/MS, Py/TMAH and FTIR. J. Anal. Appl. Pyr. 79: 39–46.

Dobrică I, Bugheanu P, Stănculescu I & Ponta C. 2008. FTIR spectral data of wood used in Romanian traditional village constructions. Ann. Univ. Buc. Chim. 17: 33–37.

Donoghue MJ. 2005. Key innovations, convergence, and success: macroevolutionary lessons from plant phylogeny. Paleobiology 31: 77–93.

Dorado J, Almendros G, Camarero S, Martínez AT, Vares T & Hatakka A. 1999. Transformation of wheat straw in the course of solid-state fermentation by four ligninolytic basidiomycetes. Enzyme and Microbial Technology 25: 605–612.

Dubois M, Gilles KA, Hamilton P, Rebers PA & Smith F. 1956. Colorimetric method of determination of sugars and related substances. Anal. Chem. 25: 350–356.

Dute RR & Evert RF. 1977. Sieve-element ontogeny in the root of *Equisetum hyemale*. Amer. J. Bot. 64: 421–438.

Dute RR, Rushing AE & Freeman JD. 1992. Survey of intervessel pit membrane structure in *Daphne* species. IAWA Bull. n.s. 13: 113–123.

Espiñeira Illobre JM. 2008. Caracterización de las ligninas de helechos y estudio de sus relaciones filogenéticas con otras plantas vasculares terrestres. Tesis Doctoral. Facultade de Ciencias Departamento de Bioloxía Animal, BioloxíaVexetal e Ecoloxía, Universidade da Coruña.

Espiñeira JM, Novo Uzal E, Gómez Ros LV, Carrión JS, Merino F, Ros Barceló A & Pomar F. 2011. Distribution of lignin monomers and the evolution of lignification among lower plants. Plant Biology 13: 59–68.

Evert RF. 2006. Esau's Plant anatomy: meristems, cells, and tissues of the plant body: their structure, function, and development. John Wiley & Sons, Inc., New Jersey.

Filisetti-Cozzi TM & Carpita N. 1991. Measurement of uronic acids without interference from neutral sugars. Anal. Biochem. 197: 157–162.

Friedman WE & Cook ME. 2000. The origin and early evolution of tracheids in vascular plants: Integration of palaeobotanical and neobotanical data. Philos. Trans. Roy. Soc. London 355: 857–868.

Gifford EM & Foster AS. 1989. Morphology and evolution of vascular plants. W.H. Freeman & Co., New York.

Gunning BES. 1977. Transfer cells and their roles in transport of solutes in plants. Sci. Prog. 64: 539–568.

Hinterstoisser B, Jalkanen R, Nowotny M & Schwanninger M. 2001. Lignification of Scots pine trees from Arctic Circle up to timberline. Buvísindi Icel. Agr. Sci. 14: 55–59.

Jansen S, Pletsers A & Sano Y. 2008. The effect of preparation techniques on SEM-imaging of pit membranes. IAWA J. 29: 161–178.

Jansen S, Smets E. & Baas P. 1998. Vestures in woody plants: a review. IAWA J. 19: 347–382.

Jeffrey EC. 1917. The anatomy of woody plants. The University of Chicago Press, Chicago.

Johansen DA. 1940. Plant microtechnique. McGraw-Hill Book Co., New York.

Kawamura I & Higuchi T. 1964. Studies on the properties of lignins of plants in various taxonomical positions. II. On the I.R. absorption spectra of lignins. Mokuzai Gakkaishi 10: 200–206.

Kenrick P & Crane PR. 1997.The origin and early diversification of land plants. A cladistic study. Smithsonian Institution Press, Washington.

Logan KJ & Thomas BA. 1985. Distribution of lignin derivatives in plants. New Phytol. 99: 571–585.

Luna ML, Giudice GE & de la Sota ER. 2008. Observations on tracheary elements in *Salpichlaena* J.Sm. (Blechnaceae, Pteridophyta). Amer. Fern J. 98: 61–70.

Luna ML, Giudice GE, Ganem MA & de la Sota ER. 2010. Structure and ultrastructure of the tracheary elements of *Asplenium* (Pteridophyta) from the Yungas, Argentina. IAWA J. 31: 227–240.

Meyer FJ. 1920. Das Leitungssystem von *Equisetum arvense*. Jahrb. Wiss. Bot. 59: 263–286.

Meyer-Berthaud B, Soria A & Decombeix AL. 2010. The land plant cover in the Devonian: a reassessment of the evolution of the tree habit. Geol. Soc. London Spec. Publ. 339: 59–70.

Morrison IM. 1988. Hydrolysis of plant cell walls with trifluoroacetic acid. Phytochemistry 27: 1097–1100.

Morrow AC & Dute RR. 1998. Development and structure of pit membranes in the rhizome of the woody fern *Botrychium dissectum*. IAWA J. 19: 429–441.

Morton CV. 1959. The identification of Costa Rican *Blechnum*. Amer. Fern J. 49: 66–69.

Nardini A, Salleo S & Jansen S. 2011. More than just a vulnerable pipeline: xylem physiology in the light of ion-mediated regulation of plant water transport. J. Exp. Bot. 62: 4701–4718.

Niklas KJ. 1985. The evolution of tracheid diameter in early vascular plants and its implications on the hydraulic conductance of the primary xylem strand. Evolution 39: 1110–1122.

O'Brien TP. 1970. Further observations on hydrolysis of the cell wall in the xylem. Protoplasma 69: 1–14.

Ogura Y. 1972. Comparative anatomy of vegetative organs of the pteridophytes. Gebr. Borntraeger, Berlin.

Pittermann J, Limm E, Rico C & Christman MA. 2011. Structure–function constraints of tracheid-based xylem: a comparison of conifers and ferns. New Phytol. 192: 449–461.

Pryer KM, Schuettpelz E, Wolf PG, Schneider H, Smith AR & Cranfill R. 2004. Phylogeny and evolution of ferns (monilophytes) with a focus on the early leptosporangiate divergences. Amer. J. Bot. 91: 1582–1598.

Ramos Giacosa JP. 2008. Revisión sistemática, análisis cladístico y biogeográfico de la Sección *Lomariocycas* (J. Sm.) C.V. Morton del género *Blechnum* L. (Blechnaceae, Pteridophyta) en América. Tesis Doctoral, Facultad de Ciencias Naturales y Museo, Universidad Nacional de La Plata, La Plata, Argentina.

Ramos Giacosa JP. 2010. *Blechnum yungense* (Pteridophyta, Blechnaceae), una nueva especie de Argentina y Bolivia. Novon 20: 68–72.

Ranker TA & Haufler CH. 2008. Biology and evolution of ferns and lycophytes. Cambridge University Press, Cambridge.

Rothwell GW & Karrfalt EE. 2008. Growth, development, and systematics of ferns: Does *Botrychium* s.l. (Ophioglossales) really produce secondary xylem? Amer. J. Bot. 95: 414–423.

Saparrat MC, Fermoselle G, Stenglein S, Aulicino M & Balatti P. 2009. *Pseudocercospora griseola* causing angular leaf spot on *Phaseolus vulgaris* produces 1,8-dihydroxynaphthalene-melanin. Mycopathologia 168: 41–47.

Saparrat MC, Estevez JM, Troncozo MI, Arambarri A & Balatti P. 2010. *In-vitro* depolymerization of *Scutia buxifolia* leaf-litter by a dominant Ascomycota *Ciliochorella* sp. Int. Biodeterior. Biodegrad. 64: 262–266.

Silva GB, Ionashiro M, Carrara TB, Crivellari AC, Tiné MAS, Prado J, Carpita NC & Buckeridge MS. 2011. Cell wall polysaccharides from fern leaves: evidence for a mannan-rich Type III cell wall in *Adiantum raddianum*. Phytochemistry 72: 2352–2360.

Simpson MG. 2010. Plant systematics. Ed. 2. Elsevier Inc.

Singh RD, Bohra R & Sharma BD. 1978. Vessels in the rhizome of *Actiniopteris radiata*. Phytomorphology 28: 455–457.

Smith AR, Pryer KM, Schuettpelz E, Korall P, Schneider H & Wolf PG. 2006. A classification for extant ferns. Taxon 55: 705–731.

Sperry JS. 2003. Evolution of water transport and xylem structure. Int. J. Plant Sci. 164: S115–S127.

Stevenson TT & Fourneaux RH. 1991. Chemical methods for the analysis of sulphated galactans from red algae. Carbohydr. Res. 210: 277–298.

Veres JS. 1990. Xylem anatomy and hydraulic conductance of Costa Rican *Blechnum* ferns. Amer. J. Bot. 77: 1610–1625.

Watkins JE, Holbrook NM & Zwieniecki MA. 2010. Hydraulic properties of fern sporophytes: consequences for ecological and evolutionary diversification. Amer. J. Bot. 97: 2007–2019.

Weng JK & Chapple C. 2010. The origin and evolution of lignin biosynthesis. New Phytol. 187: 273–285.

Weng JK, Li X, Stout J & Chapple C. 2008. Independent origins of syringyl lignin in vascular plants. Proc. Natl. Acad. Sci. USA 105*:* 7887–7892.

White RA. 1961. Vessels in roots of *Marsilea*. Science 133: 1073–1074.

Accepted: 18 October 2014